Sirte University Scientific Journal (Applied Sciences) Vol. 7 (1), 15–32 June 2017

CFD Modeling of Elbow and Orifice Meters

Abdalsalam M. Muftah

Mechanical Department, Faculty of Engineering, Sirte University, Libya
E-mail: salamgader@su.edu.ly

Abstract

Elbow and Orifice meters are two of the common flow measurement systems which are used to determine the pressure difference occurring as a fluid flows change by resistance. This differential pressure exists when a flowing changes direction due to a pipe turn as in the case of Elbow meter. The pressure difference results from the centrifugal force. Since pipe elbows exists in plants and its cost is very low. However, the accuracy is very poor [2]. Due to the fine pressure measurements required for the orifice meter, small changes in the physical geometry leads to large errors in the flow meter calculation. For example, if the fluid flow rate is too large for a given orifice, cavitation can occur, causing wear on the orifice. The same would be true for fast moving fluid with solid particulates included in the flow. For this reason, an additional study was conducted on an orifice plate with a slightly enlarged orifice to determine the sensitivity of flow measurements in regards to the orifice diameter.

The purpose of this paper is to run a CFD Model (Computational Fluid Dynamics) at Elbow and Orifice meters using Solidworks Flow Simulation [1] with different pipe sizes, ranging from $4''$ *to* $12''$ *nominal diameter. The CFD Simulation will be extended to run with using different fluid viscosities, varying as air, steam, oil and water. The goal is to determine the sensitivity of flow measurements in regards to these parameters. The results will be compared to a corresponding theoretical solution to investigate how much the accuracy can be improved by changing the geometry of the pipes and fluid viscosities.*

Keywords: *Computational Fluid Dynamics (CFD), Elbow meter, Orifice meter Pressure drop, Cavitations.*

1. Theoretical Overview

1.1 Elbow meter

Elbow meter, flow measurement device, is the most widely applied in industrial and laboratory practice. Several investigations have been reported to determine the friction factor and pressure

drops in horizontal [3] and vertical [4]. The principal of operation of this device consists basically in determining the pressure difference which is measured on points at inner and outer side of elbow duct. Sometimes, instead of preparing characteristic of the device, simple algebraic relations are used derived from experimental data, it has been shown that Bernoulli's equation can be modified to relate the pressure and elevation at these pressure points by introducing a bend coefficient term C_k which varies from 1.3 to 3.2 depending on the geometry of the elbow [5].

$$C_k \frac{V^2}{2g} = \left(\frac{P_o - P_i}{\gamma}\right) + (Z_o - Z_i)$$

By setting all terms equal to V, we get

$$V = \frac{1}{\sqrt{C_k}} \sqrt{2g \left(\frac{P_o - P_i}{\gamma}\right) + (Z_o - Z_i)}$$

Then substituting this equation into the relation $Q = V * A$, we get

$$Q = \frac{A}{\sqrt{C_k}} \sqrt{2g \left(\frac{P_o - P_i}{\gamma}\right) + (Z_o - Z_i)}$$

The pressure difference (dP) can be determined by setting all terms equal to $P_o - P_i$

$$dP = \gamma \left\{ \frac{Q^2 * C_k}{2gA^2} - dZ \right\}$$

Where $dZ = Z_o - Z_i$ and $Q = \frac{\dot{m}}{\gamma}$

The pressure difference (Δp) and velocity (V) in CFD simulation can be calculated by the following equations:

$$\Delta p = \frac{Q^2 \rho D}{r A^2}$$

$$V = \sqrt{\frac{r \Delta p}{\rho D}}$$

Where r is the radius of curvature, D is pipe diameter and ρ is the flow density.

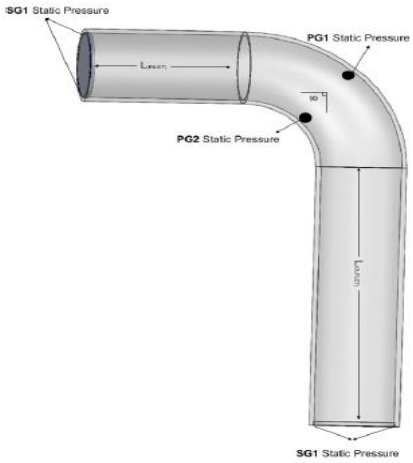

Figure 1 Elbow Meter Geometric

1.2 Orifice Meter

An orifice meter consists of an orifice plate (plate with a hole drilled in the middle) placed inside the pipe to force a moving fluid through the hole in the plate. This reduction in area causes the flow to continue to converge to a theoretical minimum flow area known as a vena contracta. By placing a pressure tap near or at the location of the vena contracta, and placing another pressure tap a short distance upstream of the orifice, it is possible to compare the differential pressure at these two locations to determine the flow rate of the fluid. A typical arrangement of the pressure taps is one nominal diameter downstream and one-half nominal diameter downstream of the orifice plate.

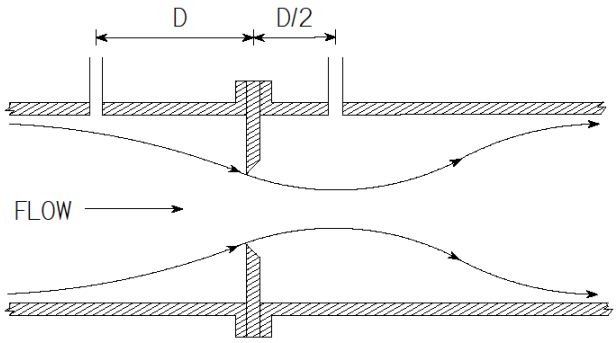

Figure 2 Orifice Meter Flow and Tap Placements

Bernoulli's equation when applied to an incompressible fluid is

$$\frac{p_1}{\gamma} + \frac{V_1^2}{2g} + z_1 = \frac{p_2}{\gamma} + \frac{V_2^2}{2g} + z_2$$

p = static pressure

γ = weight of fluid per unit volume

V = velocity

g = acceleration due to gravity

z = elevation above reference point

Q_i = ideal volumetric flow rate

Q_a = actual volumetric flow rate C_v = coefficient of velocity

A_0 = area of hole in orifice plate

C_c = contraction coefficient

C = orifice coefficient

G = mass flow rate

D_1 = pipe ID

D_2 = orifice ID

$$\beta = \frac{D_2}{D_1}$$

$$L_1 = 1 \left(for\ D\ and\ \frac{D}{2}\ taps\right)$$

$$L_2 = 0.47 \left(for\ D\ and\ \frac{D}{2}\ taps\right)$$

υ = kinematic viscosity

$$Re_D = Reynolds\ Number = \frac{V \cdot D}{\upsilon}$$

C_K = bend coefficient

Using the volumetric flow rate relation: $Q = A_1V_1 = A_2V_2$, the velocity term V_1 can be replaced in Bernoulli's equation, yielding the ideal flow rate:

$$Q_i = \frac{A_2}{\sqrt{1 - (A_2/A_1)^2}} \sqrt{2g\left(\frac{p_1}{\gamma} + z_1 - \frac{p_2}{\gamma} - z_2\right)}$$

To determine the actual flow rate, an experimentally derived coefficient is introduced into the equation to form:

$$Q_a = \frac{C_V A_2}{\sqrt{1-(A_2/A_1)^2}} \sqrt{2g\left(\frac{p_1}{\gamma} + z_1 - \frac{p_2}{\gamma} - z_2\right)}$$

Since the area of the vena contracta is actually smaller than the area of the hole in the orifice plate, a contraction coefficient is applied to the area of the hole in the orifice to derive the new A_2.

$A_2 = C_C A_0$

which can be substituted back into the previous equation to form:

$$Q_a = C A_0 \sqrt{2g\left(\frac{p_1}{\gamma} + z_1 - \frac{p_2}{\gamma} - z_2\right)}$$

Where C is derived from experimental data to form the curve fit equation:

$$C = 0.5961 + 0.0261\beta^2 - 0.216\beta^8 + 0.000521\left(\frac{10^6\beta}{Re_D}\right)^{0.7} + \left(0.0188 + 0.0063\left(\frac{19000\beta}{Re_D}\right)^{0.8}\right)\left(\frac{10^6}{Re_D}\right)^{0.3}\beta^{3.5} - 0.031\left(\frac{2L_2}{1-\beta} - 0.8\left(\frac{2L_2}{1-\beta}\right)^{1.1}\right)\beta^{1.3}$$

The mass flow rate G can be found as

$G = Q_a \gamma$

In addition, the total permanent pressure drop in the system due to the orifice restriction is also derived through experimental data, and is found to be

$\Delta P_{PL} = (1 - 0.24\beta - 0.52\beta^2 - 0.16\beta^3).(P_1 - P_2)$

2. CFD Model Geometry and Parameters

2.1 Orifice Meter Model Geometry

For the five different analyses run on the Orifice Meter, standard ANSI pipe sizes were used from $4''$ *to* $12''$ pipe with Schedule 40 wall thickness. The value of β was set equal to 0.5

for all calculations. The detailed geometry of the orifice was modeled using values from the Avco Valve manufacturer's data sheet for paddle type orifice plates (found at avcovalve.com). Static pressure measurements were taken one nominal diameter upstream of the orifice and one-half diameter downstream, just inside of the pipe wall. The straight pipe section upstream of the orifice was modeled with a length of 1.5 times the nominal diameter. The downstream pipe length was set equal to six times the nominal diameter.

2.2 Elbow Meter Model Geometry

Elbows utilized on the CFD Simulation have an angle of curvature of 90^o , average curvature and nominal diameter are ranging from $6''$ *to* $12''$. in general, the curvature pipe section length was equal to 1.5 times the nominal diameter, the straight pipe section length on the inflow side was given a length of two times of nominal diameter, while the straight pipe section length on the outflow side was given a length of four times the nominal diameter. Static pressure sensors were located at inner and outer of curvature section shown in Figure (1). The described elbows are characterized by a high level of smoothness both on inner and outer surfaces.

2.3 CFD Model Parameters

Inlet Mass flow $1.0\ lb/sec$,
Outlet Environment Pressure$\sim 14.7\ Psi$,
Fluid Types are air, steam, oil and water at $68F^{o}$.
Turbulence 2%
Gravity $(elbow\ only\ 32.2 ft/sec^2)$
γ $0{,}0361\ lbm/in^3$
ν $(orifice\ only)$ $1.052 \times 10^5\ ft^2/sec$
Pipe roughness $0\ \mu.in$

3. The CFD Meshes and Convergence

The CFD Elbow Models were run successfully for all cases. The initial mesh consists of 1484×1664 cells as shown in figure (3-a). For simplicity and computational time, the mesh was initially settled at level 3. The run was converged at small computation time around 18 second

and iteration equals to 58. Since our objective to improve the accuracy to CFD Models, the meshes were refined until level 6 as shown in figure (3-b). Increasing the refining level more than level 6 never gave any improvement for the systems. A summary of these results is listed in Table 1.

The CFD Orifice Models were also run successfully for all test cases. The initial mesh for the CFD analysis was set for the smallest fluid cells to be centered around the orifice plate, with an increasingly coarse mesh as the distance from the orifice plate increased. The initial mesh is shown as Figure 4.

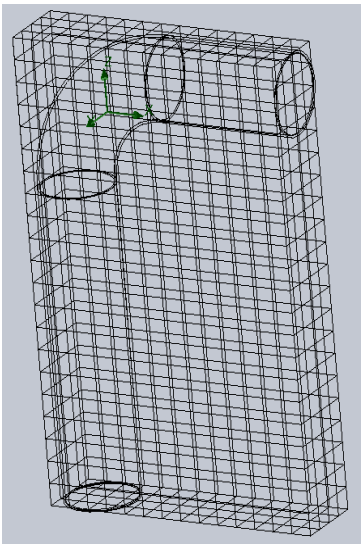

a- Initial mesh

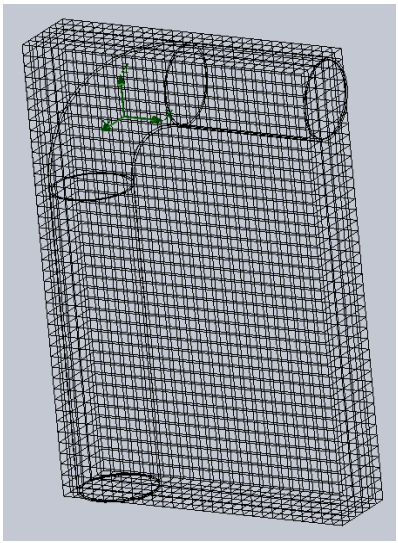

b- Final mesh

Figure 3 CFD Mesh, a) initial mesh, b) final mesh

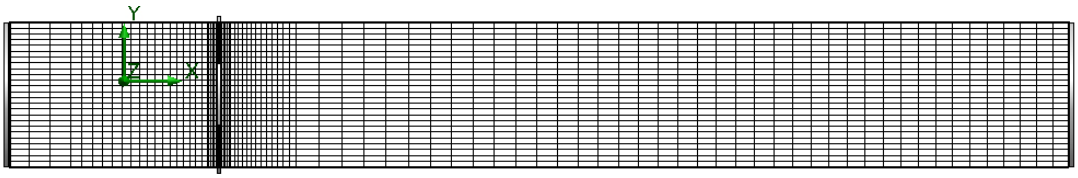

Figure 4 Initial Mesh for Orifice Meter Analysis (40,000 total fluid cells and 10,000 partial fluid cells)

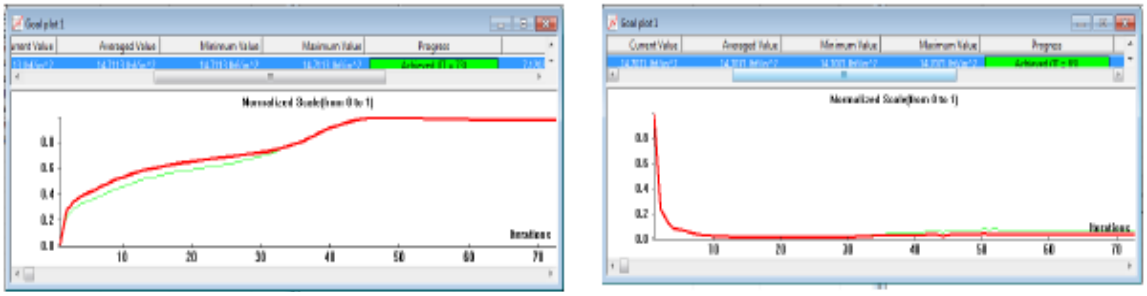

Figure 5 Samples of CFD Model Convergence

Table 1. The Refined Mesh

Elbow size	Refined mesh	Iteration
6"	12756×7496	101
8"	11872×6248	119
10"	11894×6248	83
12"	11881×6248	118

4. CFD Simulation Results

This study has been conducted on four CFD specimens with different diameter sizes varying from 4" to 12" inch, and on four CFD specimens with different liquid viscosities such as air, gas, water and oil.

4.1 CFD Results – Elbow Meter

4.1.1 CFD Model with diameter size variation:

Table 2 The sensitivity of Pressure difference to Elbow diameter size

ND	P1 - P2 (psi) Model	Theory	Error
6"	0.1357	0.1370	0.9 %
8"	0.1863	0.1875	0.65 %
10"	0.2291	0.2343	2.22 %
12"	0.2652	0.2740	3.2 %

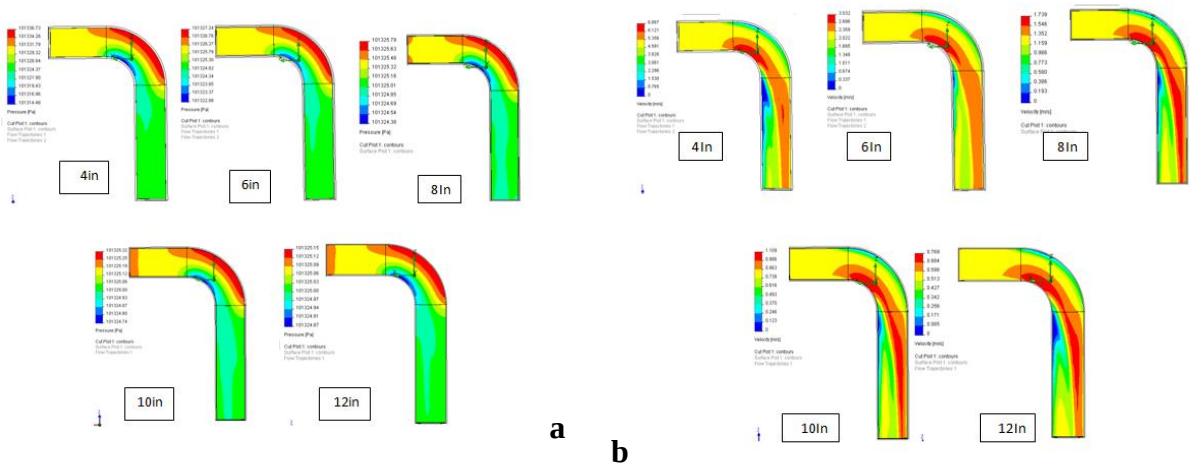

Figure 6 CFD Elbow Meter Results a) Pressure distribution b) Velocity Profile

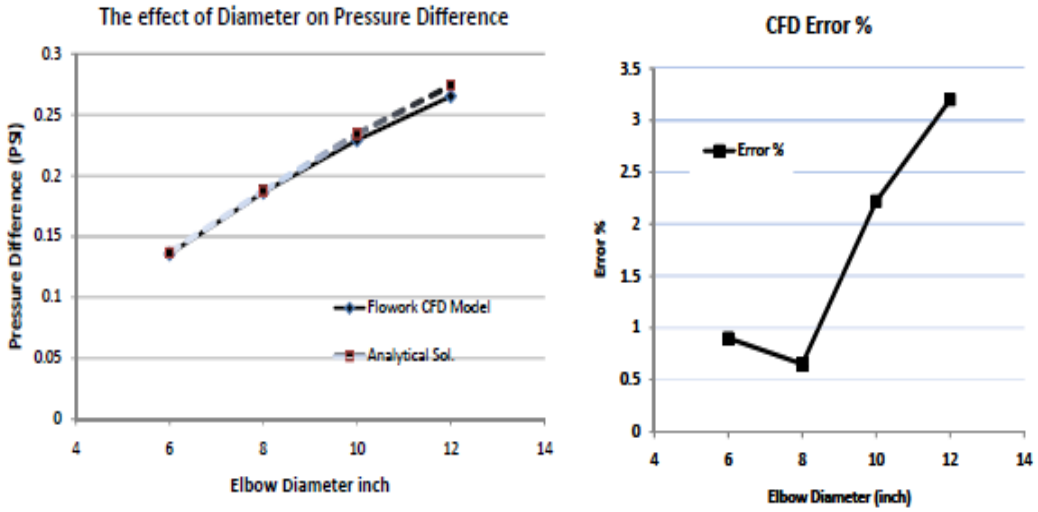

Figure 7- a) Comparison of pressure difference in CFD Models with analytical solution. b) The effect of pipe diameter on CFD Error

4.1.2 CFD Model with Fluid Viscosity variation:

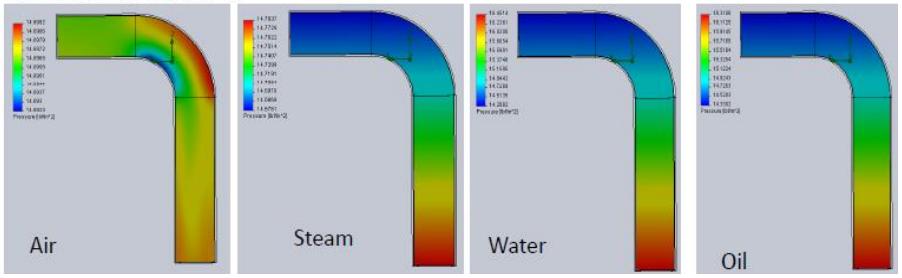

Pressure Distribution

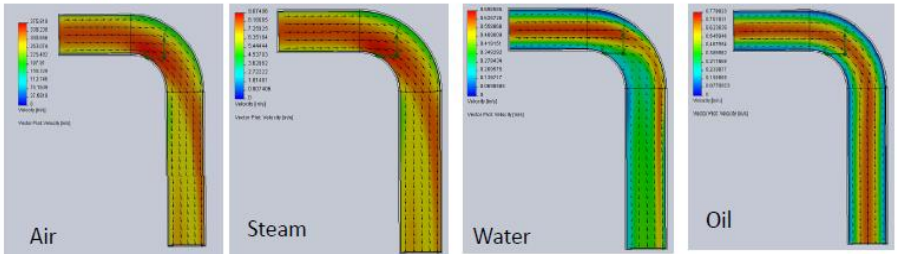

Velocity Profile

Figure 8 CFD Results a) Pressure distribution b) Velocity field

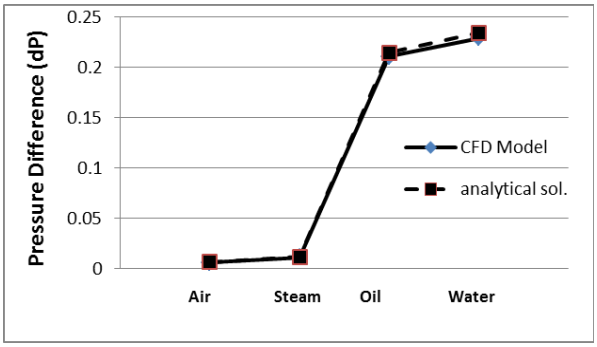

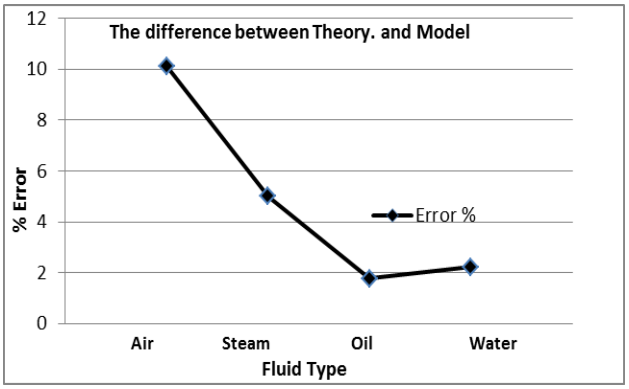

Figure 9- a) Comparison of pressure difference in CFD Models with analytical solution b) The effect of fluid type on CFD Error

Table 3 The sensitivity of Pressure difference to flow viscosity variations

ND	P1 - P2 (psi) Model	Theory	Error
Air	0.005842	0.0065	10.12 %
Steam	0.011304	0.0119	5.00 %
Oil	0.210691	0.2145	1.77 %
Water	0.22906	0.2343	2.23 %

4.2 CFD Results- Orifice Meter

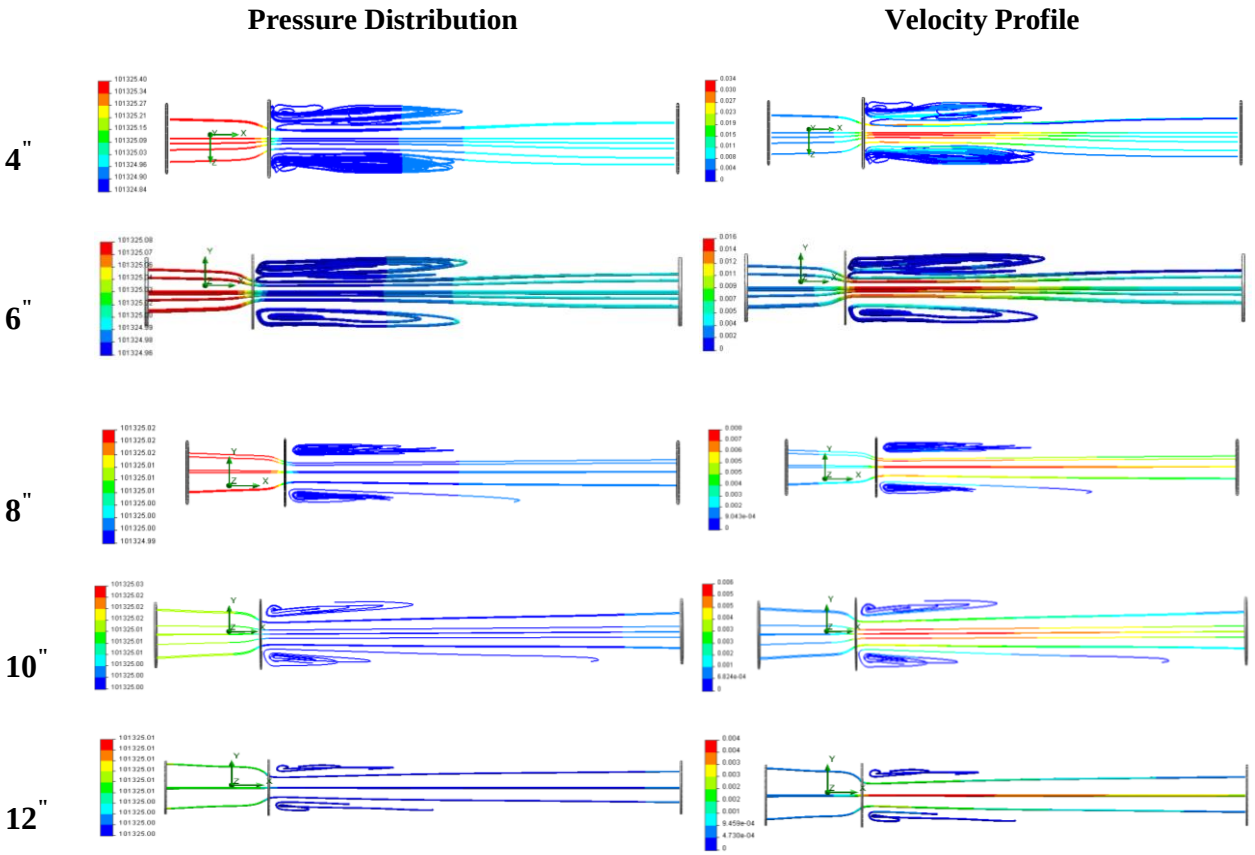

Figure 10 The effect of the diameter dimension on CFD Orifice Meter results

Table 4 The sensitivity of Pressure difference to flow viscosity variations

	P1 - P2 (psi)			Permanent Pressure Drop (psi)		
ND	Theory	Model	Error	Theory	Model	Error
4"	0.008530	0.006245	-0.2524	0.008519	0.007241	-0.1515
6"	0.001198	0.001029	-0.1524	0.001621	0.001419	-0.1274
8"	0.0003933	0.0003271	-0.2043	0.0005278	0.0004413	-0.1629
10"	0.0001557	0.0001223	-0.1668	0.0002068	0.0001817	-0.1229
12"	0.00007402	0.0000611	-0.1653	0.00009921	0.00008663	-0.1269

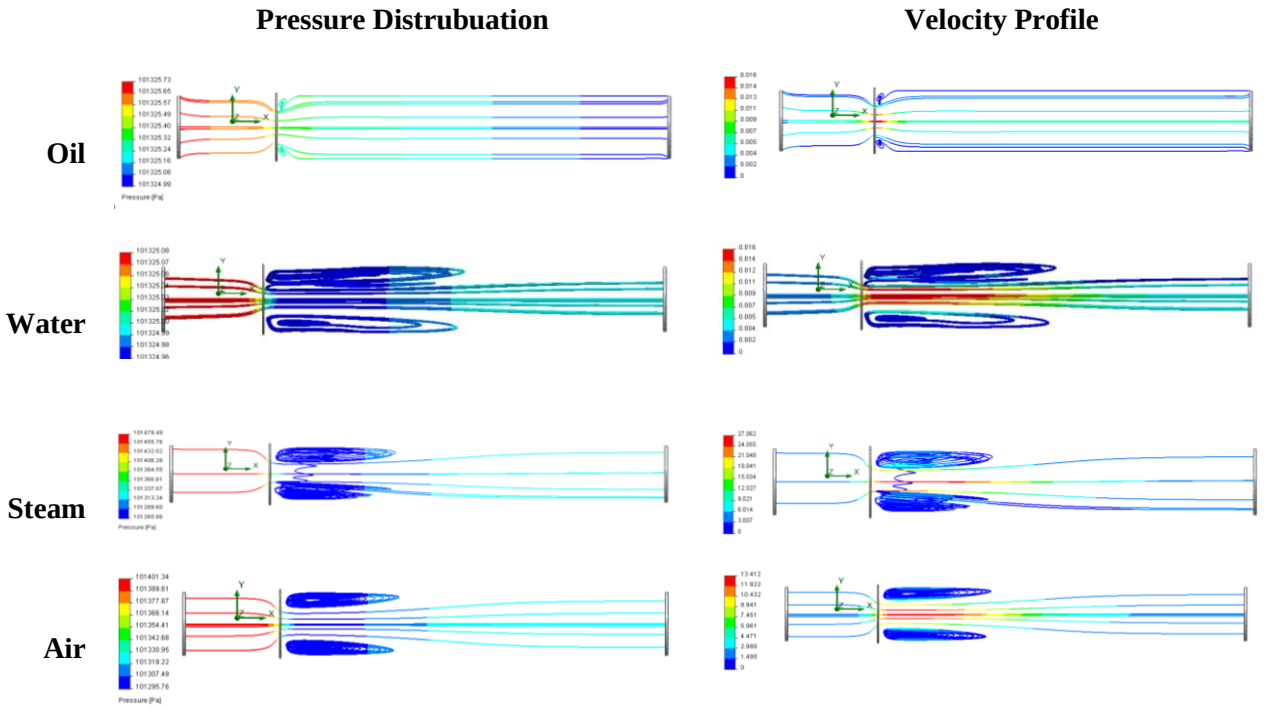

Figure 11 The effect of the fluid viscosity variation on CFD Orifice Meter results

Flow visualizations for the 4" nominal diameter configuration are shown as Figures 12, 13, and 14 above. In addition to the static pressure measurements taken at locations representing proper tap locations in the model, an additional averaged static pressure was found at the outlet of the orifice meter model which corresponded to the permanent pressure drop in the system. A

summary of the modeled and analytical results can be found in Table 4.

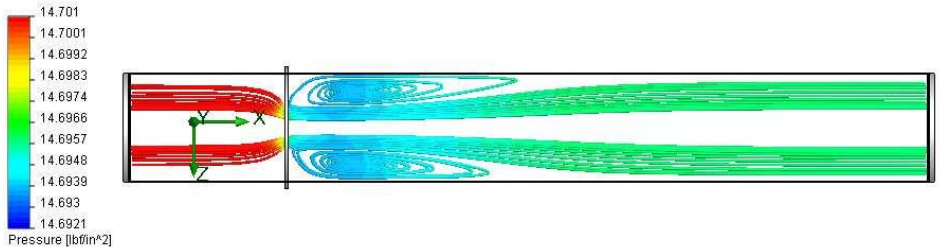

Figure 12 Water flow through 4" Orifice Meter

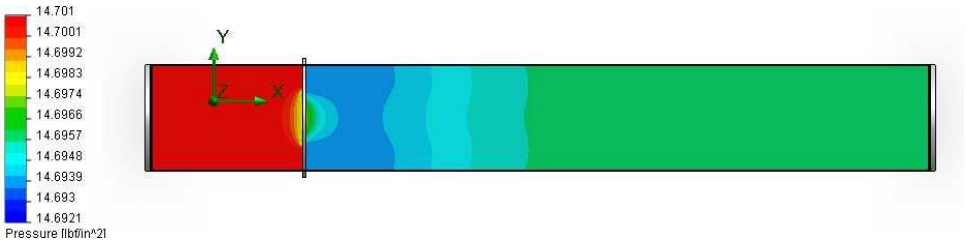

Figure 13 Pressure Distribution in 4" Orifice Meter

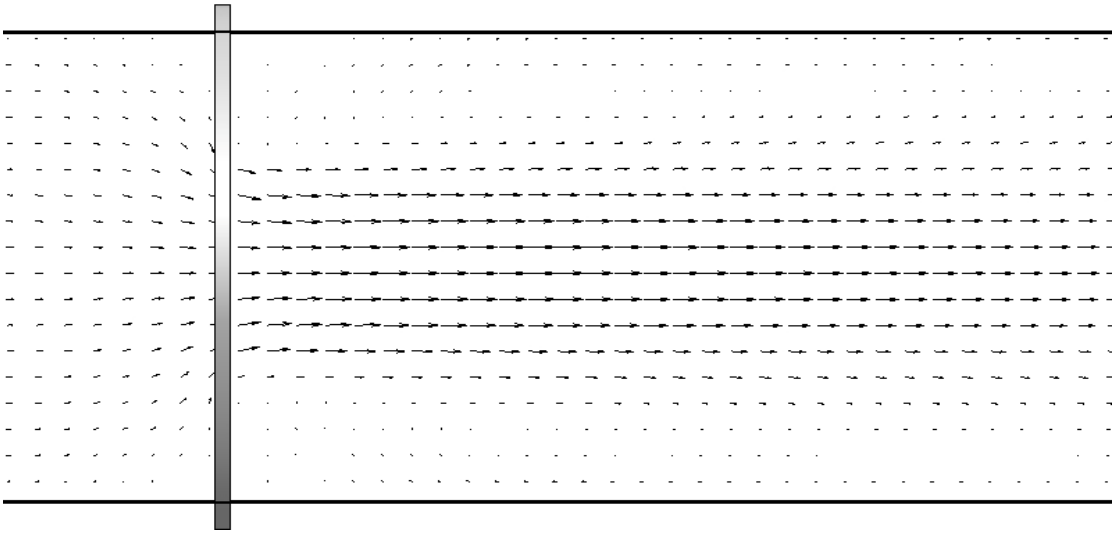

Figure 14 Gradient Field Showing Velocities through Orifice

To model wear on the orifice, an analytical calculation was made assuming that the orifice diameter was enlarged by 5%. The expected pressure difference between the taps was calculated for a mass flow rate of 1.0 lbm/sec. This pressure value was then inputted back into the analytical solution using the initial orifice diameter value in the calculations. A new

mass flow rate was found and was then compared to the 1.0 lbm/sec to determine how much of an error would be produced if the orifice diameter were enlarged by 5% without a recalibration of the meter. These results are shown below in Table 5.

Table 5 Error Produced by Gradual Wear of Orifice (5% increase in diameter)

% Error	Assuming $D_{worn} = D_{new}$	(P1 - P2) for D_{worn}	ND
-10.26	G = 0.8973 lbm/sec	0.006828 psi	4”

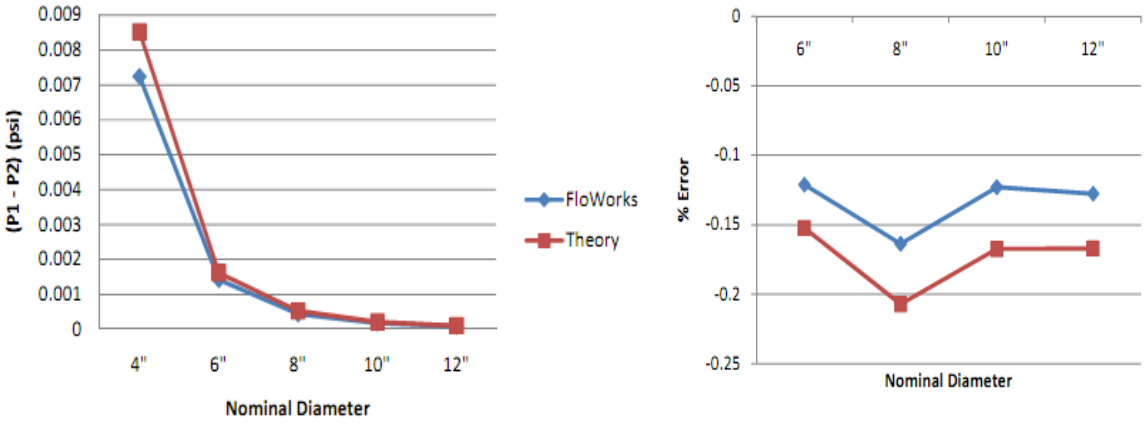

Figure 15 a) Orifice Meter Pressure Differences Found through CFD and Analytical Solutions, b) Orifice Meter CFD Percent Error

5. Cavitations

Cavitations is a phenomenon that can be present in several applications such as irrigation pressure-reducing values, sprinkler orifices or even in flow through xylem vessels inside plants. In the present study, numerical predictions of cavitation in a series of orifices were showed in CFD Flow Simulation SW. Model predictions for the orifice cases accurately capture cavitation conceptions. In general, flow simulation provides very reliable simulation for different geometries when different fluid is assumed.

According to Knapp et al (1970), cavitation can be occurred due to flow acceleration and consequently an accompanying drop pressure at a point within the liquid flow that causes vapor bubble formation. Bubbles travel downstream until the increase of pressure drop causes the

bubbles to implode. This two-step process is known as cavitation. Cavitating flows often lead to performance degradation and structural damage to many hydraulic devices.

The use of CFD in designing engineering devices has increased over the past few years due the availability of commercial codes. The effect of cavitations in circular orifices was experimentally investigated by Nurick (1976). Cavitations occur when the flow passes through a very small orifice which produces a high differential pressure. The Cavitating conditions are generated just after the orifice plates in the main line and hence the intensity of the Cavitating conditions strongly depends on the geometry of the orifice plates. When the flow passes through the orifice plates, the velocities at the orifice increase due to the sudden reduction in the area offered for the flow, resulting in decrease in the pressure. If the velocities are such that their increase is sufficient to allow the local pressure to go below the medium vapor pressure under operating conditions, cavities are formed. Such cavities are formed at downstream of the orifice plate, which also depends strongly on orifice plate cross-section, the velocities decrease giving rise to increasing pressures and pressure drops, which control the different stages of cavitations. The formed cavitations also depend strongly on the type of fluid flow passes through the orifice plate. For example, the passing air and steam flow results local pressure below the medium vapor pressure when a small change in decrease in the pressure and a small increase in velocities will be sufficient for the cavitations to occur. On the other hand, oil flow has higher vapor pressure under operating conditions, in such flow, the pressure drop often was not sufficient to let the cavitations to occur resulting stable flow.

Figure 10 shows two cycles of cavitations in downstream beyond the orifice showed unsteady situation, but after the cycles ends it reached a steady situation. The main focus of this section is to investigate the pressure drop for single phase flow in Orifice. The pressure drop in the bend was found to be dependent on the pipe diameter. CFD analysis was performed on fife different elbow size at water flow. Each of these conditions was analyzed in CFD in order to accurately predict the effect of varying the pipe diameter. Pressure contours are presented in figure (3.5). It can be seen that the pressure is higher at before throat the Orifice after troths for all pipe diameter. Figure (4.3) shows that the pressure decreased at the before throat of the pipe when

the diameter increased (Red color). Collected data in Table (6) show also that the pressure drop decreased from 0.5419497 into 0.0085537 when the pipe diameter increased from 4" to 12".

6. Discussion and Conclusion

The paper was carried out of two stages. First one was to study and investigate the sensitivity of pressure difference and distribution to the change in Elbow geometry. The results show that pressure difference increased with increasing in pipe diameter. In this paper, the error between the analytical solution and CFD outputs ranged from 0.9% to 3.2%, the larger pipe size giving larger errors. The high accuracy in present model may due to using high level of refining CFD mesh.

The second stage of this paper was to study the sensitivity of pressure difference to changing of fluid viscosity. The results show that the pressure difference increase as the fluid transmit from gas to liquid phase. The error between the analytical solution and CFD outputs ranged from 1.77% at oil to 10.12% at air. The results show that errors in Elbow meter was not depend on pipe geometric only but it also depend on the fluid which might be used. The results also recommend that in industries which used steam and liquid flow, elbow meter can give a good accuracy according to this study.

In general, the analytical method is general, systematic and significantly more accurate than computer simulations. Although Bernoulli's equation which basically used to measure the pressure loss in this paper is a simple algebraic relation, its results were not that quite consistent. For example, the result does depend on the bend coefficient term C_k which varies from 1.3 to 3.2 depending on the geometry of the pipe. This coefficient needs to be well-tested and reliable measurements are to be made. In addition, the experimental results are at considerable variance with one another in regard the best judgment of value of C_k. Generally speaking, it appears that C_k is considered not convinced especially for large pipe which no information of values has been found [5].

In this paper, it has been used this formula [1] to determine the bend coefficient C_k

$$C_k = \left[0.13 + 1.85\left(\frac{r}{R}\right)\right]\sqrt{\frac{\theta}{180}}$$

R: *Bend Radius*, r: *Pipe Radius*, θ: *Bend Angle*

Although, the effect of bends were also not considered in the CFD simulation, the results has shown a great approximation towards the analytical solution especially when the mesh has been refined. Generally speaking, it is hard to say that the analytical solution is exact solution with the observation on the bend coefficient or to say that CFD Model can give exact solution due to the computational considerations.

Although the error between the analytical results and CFD results ranged from 12-16%, a further refinement of the model did not yield better results. This error was introduced most likely because the analytical/experimental solution incorporates the orifice coefficient, C. This coefficient was initially derived by other experimenters through curve fitting physical data for a range of β. Since these physical experiments will have an inherent surface roughness associated with the physical pipe which was used, an average surface roughness value has been built in to the analytical solution. For this reason, the analytical solution predicted a greater pressure drop as was seen through the CFD analysis. Since the initial source for this experimental data is unknown, the surface roughness of the pipe used in the experiments is also unknown. If this value were given, the CFD model could be modified to include surface roughness to achieve better agreement between the analytical/experimental and CFD results.

Significant error was introduced into the analytical mass flow rate calculations by introducing a small change in the size of the orifice (5% increase in diameter). Table 2 shows that for a 4" Orifice Meter configuration, the flow measurements would be off by approximately 10%. This confirms what is often seen in industrial applications, which is that as the orifice becomes worn over time, the measurements of the flow meter produce increasingly poor results.

Lastly, the study concludes that most inline flow measurement devices require a calibration stage in order to determine a more accurate measurement for flow. The CFD analysis stresses

the importance of these calibrations, since even the slightest difference between actual and expected physical features will yield significant errors in the flow calculations. In addition, the values for the bend coefficient and the orifice coefficient are often difficult to extrapolate from previous experimental results, and differences in geometries and pipe roughness only add to the potential error of the flow rate calculations. Conducting field calibrations will significantly reduce these errors by determining device-specific coefficients to be used in the calculations.

References

[1] Mutsson J. E. (2011). An introduction to Solidworks Flow Simulation 2011, SDC Publications

[2] Figliola R. S. and Beasley D. E. (2011). Theory and Design for Mechanical Measurements, Fifth Edition, Wiley Publication.

[3] Cole J. S., Donnelly G. F., and Spedding P. L.(2004). Friction factors in two phase horizontal pipe flow, International Communications in Heat and Mass Transfer, vol. 31, no. 7, pp. 909–917.

[4] Wongwises S. and Kongkiatwanitch W.(2001). Interfacial friction factor in vertical upward gas-liquid annular two-phase flow," International Communications in Heat and Mass Transfer, vol. 28, no. 3, pp. 323–336.

[5] Pritchard P. J. and Leylegain J. C. (2011). Introduction to Fluid Mechanics, Fifth Edition, Wiley Publication.

[6] Abdalsalam M. Muftah (2014). 3D Fluid flow in an Elbow Meter-CFD Model. Sirte University Scientific Journal 4(1):35-42.

.